

# $\ell W \nu$ production at CLIC: a window to TeV scale non-decoupled neutrinos

F. del Águila

*Departamento de Física Teórica y del Cosmos and Centro Andaluz de Física de  
Partículas elementales (CAFPE),  
Universidad de Granada, E-18071 Granada, Spain*

J. A. Aguilar–Saavedra

*Departamento de Física and CFTP,  
Instituto Superior Técnico, P-1049-001 Lisboa, Portugal*

## Abstract

We discuss single heavy neutrino production  $e^+e^- \rightarrow N\nu \rightarrow \ell W\nu$ ,  $\ell = e, \mu, \tau$ , at a future high energy collider like CLIC, with a centre of mass energy of 3 TeV. This process could allow to detect heavy neutrinos with masses of 1–2 TeV if their coupling to the electron  $V_{eN}$  is in the range 0.004–0.01. We study the dependence of the limits on the heavy neutrino mass and emphasise the crucial role of lepton flavour in the discovery of a positive signal at CLIC energy. We present strategies to determine heavy neutrino properties once they are discovered, namely their Dirac or Majorana character and the size and chirality of their charged current couplings. Conversely, if no signal is found, the bound  $V_{eN} \leq 0.002 - 0.006$  would be set for masses of 1–2 TeV, improving the present limit up to a factor of 30. We also extend previous work examining in detail the flavour and mass dependence of the corresponding limits at ILC, as well as the determination of heavy neutrino properties if they are discovered at this collider.

## 1 Introduction

The existence of heavy neutrinos is usually associated to the see-saw mechanism [1], which provides a simple and elegant explanation for the smallness of light neutrino

masses. This economical solution has no phenomenological implications at large colliders, however, because the new neutrinos are extremely heavy, with masses of the order of  $10^{14}$  GeV for Yukawa couplings  $Y$  of order one. These extra neutrinos also supply a mechanism to explain the observed baryon asymmetry of the universe through leptogenesis [2]. Many attempts have been made to construct viable models of this type but with neutrino masses at the TeV scale [3, 4]. The price to pay in all cases is the loss of simplicity. Heavy neutrinos give contributions to light neutrino masses of the order  $Y^2 v^2/m_N$ , where  $v$  is the vacuum expectation value of the Higgs boson and  $m_N$  the heavy neutrino mass. These contributions are far too large for  $m_N$  in the TeV range unless (i)  $Y$  is very small, of order  $10^{-5}$ , in which case the heavy neutrino is almost decoupled from the rest of the fermions, or (ii) there is another source for neutrino masses giving a comparable contribution cancelling the  $\sim Y^2 v^2/m_N$  one from the see-saw mechanism.

Both solutions require a theoretical effort so as to build a natural model which reproduces light neutrino masses. In the first case, it is necessary to justify why neutrino Yukawa couplings are much smaller than for charged leptons and quarks. In the latter, not only it is necessary to provide an additional source of neutrino masses, but it is also crucial to give a natural explanation for the (apparently fine-tuned) cancellation of both contributions [5]. But despite the disadvantage of complexity there is the significant benefit that these models, experimentally not excluded, might be directly testable at future colliders by searching for the production of heavy neutrinos. (Additionally, there could be indirect evidence of their presence in neutrino oscillation experiments [6].) An important question is then whether these heavy states are indeed observable or not. Although their masses are within the reach of forthcoming or planned colliders, their mixing with the Standard Model (SM) leptons must be also large enough to allow for their production at detectable rates. This is because they are SM singlets, and in the absence of new interactions their couplings are proportional to their mixing with the light neutrinos.

Independently of the mass generation mechanism, heavy neutrinos with masses of several hundreds of GeV appear in Grand Unified Theories, like for instance in those based on SO(10) or on larger groups as E(6) [7], and can survive to low energies [8]. Kaluza-Klein towers of neutrinos are also predicted in models with large extra dimensions, being possible to have the first heavy modes near the electroweak scale [9]. Their existence is allowed by low energy data, which set strong constraints on their mixing with the light leptons but leave room for their production and discovery at

large colliders. If they have masses up to 400 GeV and a mixing with the electron  $V_{eN} \sim 0.01$ , they will be discovered at an international linear collider (ILC) with a centre of mass (CM) energy of 500 GeV [10]. An eventual ILC upgrade to 800 GeV will extend the reach to higher masses, but in order to experimentally test the existence of TeV scale neutrinos a larger CM energy is required, which is achievable only at a future  $e^+e^-$  collider in the multi-TeV range, like the compact linear collider (CLIC) with a CM energy of 3 TeV [11, 12].

In this paper we present a study of the CLIC potential to discover heavy neutrino singlets and determine their properties in the process  $e^+e^- \rightarrow N\nu \rightarrow \ell W\nu$ . In section 2 we review the formalism and derive the interactions of heavy Dirac and Majorana neutrino singlets with the gauge and Higgs bosons, summarising present constraints on their couplings to the charged leptons. In section 3 we discuss the general characteristics of  $eW\nu$ ,  $\mu W\nu$  and  $\tau W\nu$  final states. We analyse the different contributions to the signal and background, stressing the crucial fact that an  $eNW$  coupling is necessary to observe the heavy neutrino in any of the channels. In section 4 we describe the procedure used for our Monte Carlo calculations. The sensitivity and limits on charged current couplings achieved at CLIC are discussed in section 5, examining also the dependence on  $m_N$ . In case that a heavy neutrino was discovered, we show how its Dirac or Majorana nature could be established and its charged couplings measured. In section 6 we perform a similar analysis for neutrinos with masses of 200 – 400 GeV at ILC, extending previous work [10], also studying the determination of their properties and comparing with CLIC results. In section 7 we draw our conclusions.

## 2 Addition of neutrino singlets

In this paper we consider a SM extension with heavy Majorana (M) or Dirac (D) neutrino singlets. The most common situation is that three additional heavy eigenstates  $N_i$ ,  $i = 1, 2, 3$  are introduced, and for definiteness this is what we assume in this section. The formalism is however general for any number of singlets [14]. In the following we will obtain the interactions of heavy neutrinos with the light leptons, pointing out the differences between the Dirac and Majorana cases when they exist.

The neutrino weak isospin  $T_3 = 1/2$  eigenstates  $\nu'_{iL}$  are the same as in the SM. In the case of Dirac neutrinos we introduce 9 additional  $SU(2)_L$  singlet fields

$$N'_{iL}, \quad \nu'_{iR}, N'_{iR}, \quad i = 1, 2, 3, \quad (\text{D}) \quad (1)$$

which allow the light neutrinos to have Dirac masses too. For Majorana neutrinos only three fields are added

$$N'_{iR}, \quad i = 1, 2, 3, \quad (\text{M}) \quad (2)$$

with  $\nu'_{iR} \equiv (\nu'_{iL})^c$ ,  $N'_{iL} \equiv (N'_{iR})^c$ . In matrix notation, the form of the mass terms in the Lagrangian is similar in both cases,

$$\begin{aligned} \mathcal{L}_{\text{mass}} &= - (\bar{\nu}'_L \bar{N}'_L) \begin{pmatrix} \frac{v}{\sqrt{2}} Y' & \frac{v}{\sqrt{2}} Y \\ B' & B \end{pmatrix} \begin{pmatrix} \nu'_R \\ N'_R \end{pmatrix} + \text{H.c.}, \quad (\text{D}) \\ \mathcal{L}_{\text{mass}} &= -\frac{1}{2} (\bar{\nu}'_L \bar{N}'_L) \begin{pmatrix} M_L & \frac{v}{\sqrt{2}} Y \\ \frac{v}{\sqrt{2}} Y^T & M_R \end{pmatrix} \begin{pmatrix} \nu'_R \\ N'_R \end{pmatrix} + \text{H.c.}, \quad (\text{M}) \quad (3) \end{aligned}$$

where the  $Y$ ,  $B$  and  $M$  blocks are  $3 \times 3$  matrices.<sup>1</sup> The physical meaning is of course different, since the  $Y$  matrices correspond to Yukawa interactions,  $B$ ,  $B'$  are bare mass terms and  $M_L$ ,  $M_R$  lepton number violating Majorana mass matrices.<sup>2</sup> The complete mass matrices  $\mathcal{M}$  can be diagonalised by  $\mathcal{U}_L^\dagger \mathcal{M} \mathcal{U}_R = \mathcal{M}_{\text{diag}}$ . For Majorana neutrinos  $\mathcal{U}_R = \mathcal{U}_L^*$ , while for Dirac neutrinos the two unitary matrices are independent. The mass eigenstates are

$$\begin{pmatrix} \nu_L \\ N_L \end{pmatrix} = \mathcal{U}_L^\dagger \begin{pmatrix} \nu'_L \\ N'_L \end{pmatrix}, \quad \begin{pmatrix} \nu_R \\ N_R \end{pmatrix} = \mathcal{U}_R^\dagger \begin{pmatrix} \nu'_R \\ N'_R \end{pmatrix}. \quad (4)$$

Both for Majorana and Dirac neutrinos the weak interaction Lagrangian is written in the weak eigenstate basis as

$$\begin{aligned} \mathcal{L}_W &= -\frac{g}{\sqrt{2}} \bar{l}'_L \gamma^\mu \nu'_L W_\mu + \text{H.c.}, \\ \mathcal{L}_Z &= -\frac{g}{2c_W} \bar{\nu}'_L \gamma^\mu \nu'_L Z_\mu, \end{aligned} \quad (5)$$

---

<sup>1</sup>Both mass terms in Eqs. (3) are particular cases of a general  $12 \times 12$  symmetric mass matrix connecting  $(\nu'_L \ (\nu'_R)^c \ N'_L \ (N'_R)^c)$  and  $((\nu'_L)^c \ \nu'_R \ (N'_L)^c \ N'_R)$ . If we assign lepton numbers  $L = 1$  to  $\nu'_L, N'_L$  and  $L = -1$  to  $(\nu'_R)^c, (N'_R)^c$ , the mass term for Dirac neutrinos corresponds to the  $L = 0$  entries (with conserved lepton number). The mass term for Majorana neutrinos includes the Yukawa entries  $Y$  with  $L = 0$  and the diagonal lepton number violating blocks  $M_L, M_R$  with  $L = 2, L = -2$ , respectively, and in this case  $\nu'_R, N'_L$  are assumed very heavy or decoupled.

<sup>2</sup>In the Dirac case the right-handed states  $\nu'_{iR}, N'_{iR}$  are equivalent, and by a suitable redefinition one can always choose a weak basis with  $B' = 0$ . Additionally, with adequate rotations  $B$  and  $M_R$  could be assumed diagonal without loss of generality. This is not necessary for our discussion, anyway, and the results in this section do not rely on such assumptions.

with  $l'_{iL}$  the charged lepton weak eigenstates. Let us divide for convenience the rotation matrices  $\mathcal{U}_L, \mathcal{U}_R$  in  $3 \times 6$  blocks,

$$\mathcal{U}_L = \begin{pmatrix} U_L \\ U'_L \end{pmatrix}, \quad \mathcal{U}_R = \begin{pmatrix} U_R \\ U'_R \end{pmatrix}. \quad (6)$$

Then, the weak interaction Lagrangian is written in the mass eigenstate basis as

$$\mathcal{L}_W = -\frac{g}{\sqrt{2}} \bar{l}_L \gamma^\mu U_i^\dagger U_L \begin{pmatrix} \nu_L \\ N_L \end{pmatrix} W_\mu + \text{H.c.}, \quad (7)$$

$$\mathcal{L}_Z = -\frac{g}{2c_W} (\bar{\nu}_L \bar{N}_L) \gamma^\mu U_L^\dagger U_L \begin{pmatrix} \nu_L \\ N_L \end{pmatrix} Z_\mu, \quad (8)$$

where  $U_i$  is a  $3 \times 3$  unitary matrix resulting from the diagonalisation of the charged lepton mass matrix. The extended Maki-Nakagawa-Sakata (MNS) matrix [13]  $V \equiv U_i^\dagger U_L$  has dimension  $3 \times 6$ . Neutral interactions are described by the  $6 \times 6$  matrix  $X \equiv U_L^\dagger U_L$ , related to the former by  $X = V^\dagger V$ .

The interactions with the Higgs boson  $H$  are

$$\begin{aligned} \mathcal{L}_H &= -\frac{1}{\sqrt{2}} (\bar{\nu}'_L Y N'_R + \bar{\nu}'_L Y' \nu'_R) H + \text{H.c.}, \\ &= -\frac{1}{\sqrt{2}} (\bar{\nu}_L \bar{N}_L) U_L^\dagger (Y U'_R + Y' U_R) \begin{pmatrix} \nu_R \\ N_R \end{pmatrix} H + \text{H.c.}, \end{aligned} \quad (\text{D})$$

$$\begin{aligned} \mathcal{L}_H &= -\frac{1}{\sqrt{2}} \bar{\nu}'_L Y N'_R H + \text{H.c.} \\ &= -\frac{1}{\sqrt{2}} (\bar{\nu}_L \bar{N}_L) U_L^\dagger Y U_L^* \begin{pmatrix} \nu_R \\ N_R \end{pmatrix} H + \text{H.c.} \end{aligned} \quad (\text{M}) \quad (9)$$

In order to obtain explicit expressions in terms of masses and mixing angles, we decompose  $V$  in two  $3 \times 3$  blocks,  $V = (V^{(\nu)} \ V^{(N)})$ , with  $V^{(\nu)}, V^{(N)}$  parameterising the mixing of the charged leptons with the light and heavy neutrinos, respectively. The latter is experimentally constrained to be small (see below), thus terms of order  $(V^{(N)})^2$  can be neglected. After a little algebra, the scalar interactions of both heavy Dirac and Majorana neutrinos can be written as

$$\mathcal{L}_H = -\frac{g}{2M_W} \bar{\nu}_L V^{(\nu)\dagger} V^{(N)} M_N N_R + \text{H.c.}, \quad (10)$$

with  $M_N$  their  $3 \times 3$  diagonal mass matrix  $M_N = \text{diag}(m_{N_1}, m_{N_2}, m_{N_3})$ . In the Dirac case there are additional Yukawa couplings among the light neutrinos.

The mixing of heavy neutrinos with charged leptons is restricted by two groups of processes [15–21]: (i)  $\pi \rightarrow \ell\nu$ ,  $Z \rightarrow \nu\bar{\nu}$  and other tree-level processes involving light neutrinos in the final state; (ii)  $\mu \rightarrow e\gamma$ ,  $Z \rightarrow \ell^+\ell'^-$  and other lepton flavour violating (LFV) processes to which heavy neutrinos can contribute at one loop level. All these processes constrain the quantities

$$\Omega_{\ell\ell'} \equiv \delta_{\ell\ell'} - \sum_{i=1}^3 V_{\ell\nu_i} V_{\ell'\nu_i}^* = \sum_{i=1}^3 V_{\ell N_i} V_{\ell' N_i}^*. \quad (11)$$

The processes in the first group measure lepton charged current couplings. A global fit yields the bounds [20]

$$\Omega_{ee} \leq 0.0054, \quad \Omega_{\mu\mu} \leq 0.0096, \quad \Omega_{\tau\tau} \leq 0.016, \quad (12)$$

with a 90% confidence level (CL). For heavy neutrino masses in the TeV range, LFV processes in the second group give the constraints [19]

$$|\Omega_{e\mu}| \leq 0.0001, \quad |\Omega_{e\tau}| \leq 0.01, \quad |\Omega_{\mu\tau}| \leq 0.01. \quad (13)$$

The limits in Eqs. (12) are model-independent to a large extent, and independent of heavy neutrino masses as well. They imply that the mixing of the heavy eigenstates with the charged leptons is very small,  $\sum_i |V_{\ell N_i}|^2 \leq 0.0054, 0.0096, 0.016$  for  $\ell = e, \mu, \tau$ , respectively. On the other hand, the bounds in Eqs. (13) do not directly constrain the products  $V_{\ell N_i} V_{\ell' N_i}^*$  but the sums in the r.h.s. of Eq. (11), and cancellations might occur between two or more terms, and also with other new physics contributions. These cancellations may be more or less natural, but in any case such possibility makes the limits in Eqs. (13) relatively weak if more than one heavy neutrino exists [10, 22]. Besides, we note that these limits are independent of the heavy neutrino nature. For heavy Majorana neutrinos there is an additional restriction from the non-observation of neutrinoless double beta decay, which is below present experimental limits for  $|V_{eN}|^2 \leq 0.0054$  and  $m_{N_i} \gtrsim 100$  GeV [23].

Since mixing of the charged leptons with heavy neutrinos is experimentally required to be very small, the usual MNS matrix  $V^{(\nu)}$  is approximately unitary, up to corrections of order  $V_{\ell N_i}^2$ . Moreover, at large collider energies the light neutrino masses can be neglected. With these approximations  $V^{(\nu)}$  can be taken equal to the identity matrix, implying also  $X_{\nu\ell\nu\ell'} = \delta_{\ell\ell'}$ ,  $X_{\nu\ell N_i} = V_{\ell N_i}$ , *i.e.* the vertices between light leptons can be taken equal to their SM values for massless neutrinos, and the couplings for flavour-changing neutral interactions  $\nu_\ell N_i Z$  are proportional to those for charged currents  $\ell N_i W$ .

The production of a heavy neutrino  $N$  involves its interactions with the light fermions. The charged current vertex with a charged lepton  $\ell$  can be directly read from Eq. (7),

$$\mathcal{L}_W = -\frac{g}{\sqrt{2}} (\bar{\ell}\gamma^\mu V_{\ell N} P_L N W_\mu + \bar{N}\gamma^\mu V_{\ell N}^* P_L \ell W_\mu^\dagger). \quad (14)$$

The neutral current gauge couplings with a light neutrino  $\nu_\ell$  are

$$\mathcal{L}_Z = -\frac{g}{2c_W} (\bar{\nu}_\ell\gamma^\mu V_{\ell N} P_L N + \bar{N}\gamma^\mu V_{\ell N}^* P_L \nu_\ell) Z_\mu. \quad (15)$$

In the Dirac case, the two terms in  $\mathcal{L}_Z$  describe the interactions of heavy neutrinos and antineutrinos. If they are Majorana particles, the second term can be rewritten in terms of  $\bar{\nu}_\ell$  and  $N$ , giving

$$\mathcal{L}_Z = -\frac{g}{2c_W} \bar{\nu}_\ell\gamma^\mu (V_{\ell N} P_L - V_{\ell N}^* P_R) N Z_\mu. \quad (\text{M}) \quad (16)$$

The scalar interactions of the heavy neutrino are

$$\mathcal{L}_H = -\frac{g m_N}{2M_W} (\bar{\nu}_\ell V_{\ell N} P_R N + \bar{N} V_{\ell N}^* P_L \nu_\ell) H, \quad (17)$$

where the second term can again be rewritten for Majorana neutrinos,

$$\mathcal{L}_H = -\frac{g m_N}{2M_W} \bar{\nu}_\ell (V_{\ell N} P_R + V_{\ell N}^* P_L) N H. \quad (\text{M}) \quad (18)$$

For our computations it is also necessary to know the total heavy neutrino width  $\Gamma_N$ .  $N$  can decay in the channels  $N \rightarrow W^+ \ell^-$  (if  $N$  is a Majorana fermion  $N \rightarrow W^- \ell^+$  is allowed as well),  $N \rightarrow Z \nu_\ell$  and  $N \rightarrow H \nu_\ell$ . The partial widths for these decays are [22, 24]

$$\begin{aligned} \Gamma(N \rightarrow W^+ \ell^-) &= \Gamma(N \rightarrow W^- \ell^+) \\ &= \frac{g^2}{64\pi} |V_{\ell N}|^2 \frac{m_N^3}{M_W^2} \left(1 - \frac{M_W^2}{m_N^2}\right) \left(1 + \frac{M_W^2}{m_N^2} - 2\frac{M_W^4}{m_N^4}\right), \\ \Gamma_D(N \rightarrow Z \nu_\ell) &= \frac{g^2}{128\pi c_W^2} |V_{\ell N}|^2 \frac{m_N^3}{M_Z^2} \left(1 - \frac{M_Z^2}{m_N^2}\right) \left(1 + \frac{M_Z^2}{m_N^2} - 2\frac{M_Z^4}{m_N^4}\right), \\ \Gamma_M(N \rightarrow Z \nu_\ell) &= 2\Gamma_D(N \rightarrow Z \nu_\ell), \\ \Gamma_D(N \rightarrow H \nu_\ell) &= \frac{g^2}{128\pi} |V_{\ell N}|^2 \frac{m_N^3}{M_W^2} \left(1 - \frac{M_H^2}{m_N^2}\right)^2, \\ \Gamma_M(N \rightarrow H \nu_\ell) &= 2\Gamma_D(N \rightarrow H \nu_\ell), \end{aligned} \quad (19)$$

with  $\Gamma_D$  and  $\Gamma_M$  standing for the widths of a Dirac and Majorana neutrino. The factors of two in the partial widths of  $N \rightarrow Z\nu_\ell$ ,  $N \rightarrow H\nu_\ell$  for a Majorana neutrino are the consequence of the extra  $V_{\ell N}^*$  couplings in Eqs. (16),(18), which are not present for a Dirac neutrino. From Eqs. (19) it follows that for equal values of the mixing angles  $V_{\ell N}$  the width of a heavy Majorana neutrino is twice as large as for a Dirac neutrino. Another straightforward consequence of these expressions is that the partial widths for  $W$ ,  $Z$  and Higgs decays are in the ratios 2 : 1 : 1 (the latter for  $m_H \ll m_N$ ). Since the Higgs mass is still unknown, we will ignore the decays  $N \rightarrow H\nu_\ell$  in the calculation of  $\Gamma_N$ . If these decays are included, the  $W^\pm\ell^\mp$  branching ratios (and hence the final signal cross sections) are multiplied by a factor which ranges between 3/4 (for  $m_H \ll m_N$ ) and unity (for  $m_H \geq m_N$ ).

### 3 $\ell W\nu$ production and lepton flavour

The existence of new heavy neutrinos is rather difficult to detect as an excess in the total cross section for  $e^+e^- \rightarrow \ell q\bar{q}'\nu$ . The stringent experimental bounds on their mixing angles with the light particles restrict the size of their contribution to this process to a few percent, except for low  $m_N$  values. Such a small increase in the cross section is unobservable due to the inherent uncertainties in the SM prediction. Nevertheless, the heavy neutrino contribution to this signal is dominated by on-shell  $N$  production [22, 25]  $e^+e^- \rightarrow N\nu \rightarrow \ell^-W^+\nu \rightarrow \ell^-q\bar{q}'\nu$  (plus the charge conjugate) if kinematically accessible, yielding a peak in the  $\ell q\bar{q}'$  invariant mass distribution. If heavy neutrino mass differences are of the order of 100 GeV or more the neutrino peaks do not overlap, so that their experimental study can be done independently, since in this case the interference of the relevant amplitudes is negligible. We will thus assume for simplicity that only one heavy neutrino  $N$  is produced. For quasidegenerate heavy neutrinos with  $(m_{N_1} - m_{N_2})/(m_{N_1} + m_{N_2}) \ll 1$  [4] one must consider interference effects, which are not addressed here.

In  $N\nu$  production the two quarks in the final state result from the decay of an on-shell  $W$  boson, hence we can safely confine the analysis to the phase space region where their invariant mass is not far from  $M_W$ , and restrict the calculation to  $\ell W\nu$  production (with  $W \rightarrow q\bar{q}'$ ) in the presence of a heavy neutrino. We first discuss the process for  $\ell = e$  and later point out the differences for  $\ell = \mu, \tau$ , using a reference value  $m_N = 1500$  GeV. For most purposes  $\ell^-$  and  $\ell^+$  production may be summed because CP-violating effects are negligible, as it is briefly commented at the end of this section.



### 3.1 Final states with electrons

The Feynman diagrams for  $e^+e^- \rightarrow e^-W^+\nu$  involving heavy neutrino exchange are shown in Fig. 1. We neglect the electron mass (as well as light quark masses) in the computation of matrix elements, thus we do not include scalar diagrams. When the outgoing light neutrino flavour is constrained to be  $\nu_e$  we write it explicitly. Diagrams 1b and 1f are present only if  $N$  is a Majorana fermion, while the rest are common to the Dirac and Majorana cases.

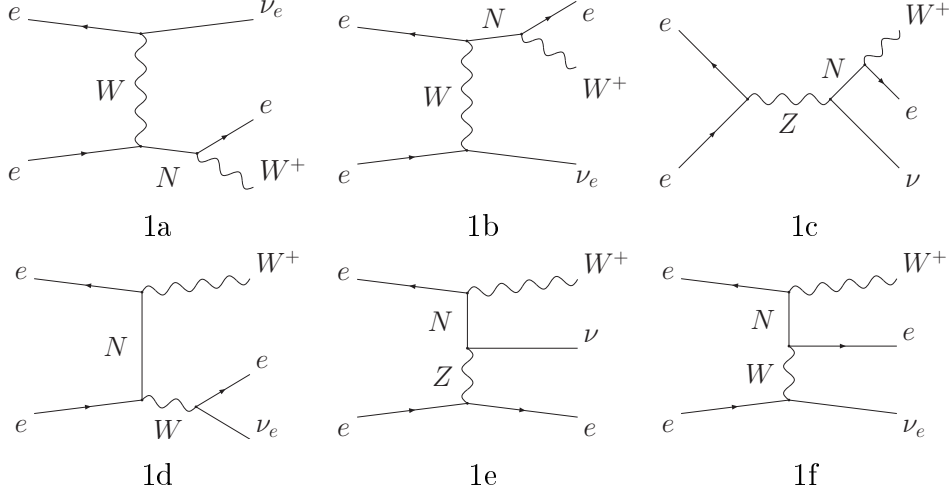


Figure 1: Feynman diagrams for  $e^+e^- \rightarrow e^-W^+\nu$  mediated by a heavy neutrino  $N$ . The differences between the Dirac and Majorana cases are discussed in the text.

We notice that the six diagrams have an  $eNW$  vertex, whose presence is thus necessary for this process to occur. The three first ones involve the production of on-shell  $N$ , the corresponding amplitudes being proportional to  $V_{eN}$  times a factor  $O(1)$  from the  $N$  decay branching ratio. Their contribution to the cross section is then quadratic in  $V_{eN}$  (interference with the SM amplitude is negligible). The last three diagrams are proportional to  $V_{eN}^2$ , giving  $V_{eN}^2$  terms in the cross section (through interference), plus  $V_{eN}^4$  terms. With present limits on  $V_{eN}$ , the former are one order of magnitude larger than the latter, but still remain two orders of magnitude below the size of  $V_{eN}^2$  terms from diagrams with  $N$  on its mass shell. Among these, the  $t$ - and  $u$ -channel  $W$  exchange diagrams (1a and 1b, respectively) are the only ones relevant at CLIC energy and  $s$ -channel  $Z$  exchange (1c) is highly suppressed, being a factor  $\sim 5$  smaller than off-shell contributions. We then arrive to one crucial point: for equal values of the mixing angles, the contributions of Majorana and Dirac heavy neutrinos

to the  $e^-q\bar{q}'\nu$  cross section are almost equal. The reason is simple: for a Majorana  $N$  the neutrino signal is strongly dominated by two non-interfering Feynman diagrams which give equal contributions to the cross section, instead of one in the Dirac case. On the other hand, the width of a Majorana  $N$  is twice as large as for a Dirac one, as noted in the previous section.

In the phase space region of interest, the relevant SM diagrams are those for  $e^+e^- \rightarrow e^-W^+\nu_e$  with subsequent hadronic  $W$  decay, as depicted in Fig. 2. The main contribution comes from diagram 2i and is one order of magnitude larger than the rest. This fact contrasts with the behaviour at ILC energy, where about one half of the cross sections comes from resonant  $W^+W^-$  production, especially from diagram 2a. The 8 additional diagrams for  $e^+e^- \rightarrow e^-q\bar{q}'\nu$  which do not involve the decay  $W^+ \rightarrow q\bar{q}'$  give an irrelevant contribution (smaller than 0.5 %) in the phase space region studied. The quadratic corrections to the  $\ell\nu W$  and  $\nu\nu Z$  vertices neglected in section 2 are unobservable with the available statistics. We also ignore diagrams like 1b and 1f with the exchange of a light Majorana neutrino, which are suppressed by the ratio  $m_\nu/Q \sim 10^{-13}$ , where  $Q \sim \sqrt{s}$  is the typical energy scale in the process.

It is worth pointing out the effect of beam polarisation on the cross sections for  $e^-W^+\nu$  production through  $N$  exchange only and through SM diagrams. For  $N$  exchange we have  $\sigma_{e_R^+e_L^-} : \sigma_{e_L^+e_R^-} = 44000 : 1$  (for  $m_N = 1500$  GeV,  $V_{eN} = 0.05$ ), with  $\sigma_{e_R^+e_R^-} = \sigma_{e_L^+e_L^-} = 0$ . For the SM process, we find  $\sigma_{e_R^+e_L^-} : \sigma_{e_L^+e_R^-} = 3700 : 200 : 1$ ,  $\sigma_{e_L^+e_L^-} = 0$ . Therefore, the use of negative electron polarisation  $P_{e^-}$  and positive positron polarisation  $P_{e^+}$  improves the observability of the signal as well as the statistics. Besides, it can be seen that  $e_L^+e_R^-$  cross sections only receive contributions from diagrams with  $Z$  or photon  $s$ -channel exchange, thus the huge difference between  $e_L^+e_R^-$  and  $e_R^+e_L^-$  cross sections reflects the suppression of the former.

### 3.2 Final states with muons and taus

Final states with  $\ell = \mu, \tau$  share similar production properties and we refer to muons for brevity. The diagrams for  $e^+e^- \rightarrow \mu^-W^+\nu$  via heavy neutrino exchange are shown in Fig. 3. The same comments regarding the contributions of the diagrams in Fig. 1 apply in this case (up to different mixing angles). We observe that all contributions except 3c involve an electron-heavy neutrino interaction; in particular, the leading diagrams 3a and 3b correspond to heavy neutrino production via an  $eNW$  vertex with subsequent decay through a  $\mu NW$  interaction. This leads to the important consequence that the

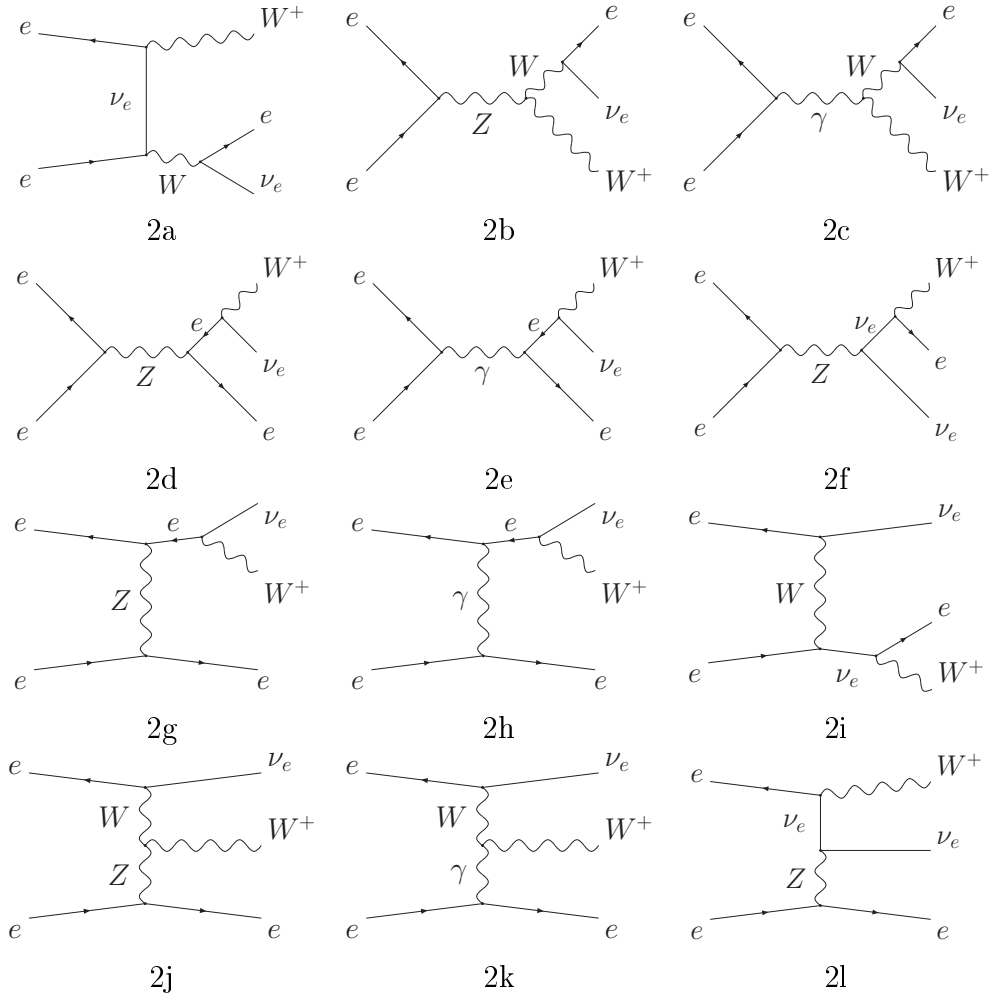


Figure 2: Feynman diagrams for  $e^+e^- \rightarrow e^-W^+\nu_e$  within the SM.

$\mu^-W^+\nu$  signal of heavy neutrinos is relevant only if  $N$  simultaneously mixes with the electron and muon. We also notice that, even without mixing with the muon, a heavy neutrino can mediate  $\mu^-W^+\nu$  production, via diagram 3d. Nevertheless, the cross section is very small in this case. The SM background is  $e^+e^- \rightarrow \mu^-W^+\nu_\mu$ , with 6 Feynman diagrams like the ones in 2a–2f but replacing  $e^-$ ,  $\nu_e$  by  $\mu^-$ ,  $\nu_\mu$ , respectively. Its cross section is dominated by resonant  $W^+W^-$  production and is 30 times smaller than for  $e^-W^+\nu_e$ .

In order to discuss the effect of beam polarisation we have to distinguish two cases. If  $\mu^-W^+\nu$  production takes place mainly through a  $eNW$  coupling, beam polarisation has clearly the same effect as in  $e^-W^+\nu$  production: negative  $P_{e^-}$  and positive  $P_{e^+}$  enhance the signal and background and thus improve the statistics. If the heavy neutrino does

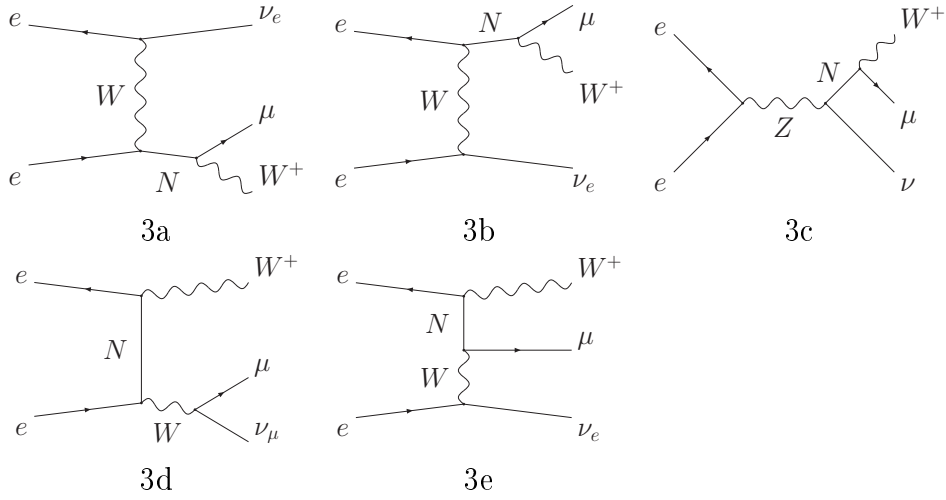


Figure 3: Feynman diagrams for  $e^+e^- \rightarrow \mu^-W^+\nu$  mediated by a heavy neutrino  $N$ . The differences between the Dirac and Majorana cases are discussed in the text.

not mix with the electron but mixes with the muon, the reverse situation occurs. Since the only contribution comes from diagram 3c, the use of left-handed positrons and right-handed electrons actually increases the signal, while reducing the SM cross section for this process [10]. This case has no interest at CLIC energy, anyway, because for  $V_{eN} = 0$  the signal is not observable.

### 3.3 CP violation with heavy neutrinos

In this work we do not address any CP violation effects, which are unobservable in the processes studied. Partial rate asymmetries between  $\ell^-$  and  $\ell^+$  final states are negligible at the tree level. They require interference of diagrams with different CP-conserving phases (*e.g.* diagram 1a, with a phase arising from the  $N$  propagator [27], and one of the diagrams in Fig. 2). This interference is very small due to kinematics (the width  $\Gamma_N$  is small compared to the energy scale). Another possibility is the study of triple-product asymmetries in the decay of the heavy neutrino. However, these asymmetries are proportional to the mass of the final state charged lepton [28], and hence very small. Therefore, we sum  $\ell^-$  and  $\ell^+$  final states in all our results, unless otherwise stated.

## 4 Event generation

The matrix elements for  $e^+e^- \rightarrow \ell^-W^+\nu \rightarrow \ell^-q\bar{q}'\nu$  are calculated using HELAS [29], including all spin correlations and finite width effects. We sum SM and heavy neutrino-mediated diagrams at the amplitude level. For Majorana fermions the Feynman rules are given in Ref. [30]. We assume a CM energy of 3 TeV, with a beam spread of 0.35% [11], ignoring an eventual beam crossing angle of 0.02 rad at the interaction point [12] whose effect in our simulation is very small. We make use of electron polarisation  $P_{e^-} = -0.8$  and positron polarisation  $P_{e^+} = 0.6$ . The luminosity is taken as  $1000 \text{ fb}^{-1}$  per year. In order to take into account the effect of initial state radiation (ISR) and beamstrahlung we convolute the differential cross section with “structure functions”  $D_{\text{ISR}}(x)$ ,  $D_{\text{BS}}(x)$ ,

$$d\sigma = \int_0^1 d\sigma(x_1y_1E, x_2y_2E)D_{\text{ISR}}(x_1)D_{\text{BS}}(y_1)D_{\text{ISR}}(x_2)D_{\text{BS}}(y_2) dx_1dy_1dx_2dy_2. \quad (20)$$

The function describing the effect of ISR used is [31]

$$D_{\text{ISR}}(x) = \frac{\eta}{2}(1-x)^{\frac{\eta}{2}-1} \frac{e^{\frac{\eta}{2}(\frac{3}{4}-\gamma)}}{\Gamma(1+\frac{\eta}{2})} \times \left[ \frac{1}{2}(1+x^2) - \frac{\eta}{8} \left( \frac{1}{2}(1+3x^2) \log x - (1-x)^2 \right) \right], \quad (21)$$

where

$$\eta(s) = -6 \log \left[ 1 - \frac{\alpha_0}{3\pi} \log \frac{s}{m_e^2} \right], \quad (22)$$

$\gamma$  is the Euler constant,  $\alpha_0 = 1/137$  the fine structure constant,  $s$  the center of mass energy squared and  $m_e$  the electron mass. For beamstrahlung we use [32]

$$D_{\text{BS}}(x) = e^{-N} \left[ \delta(x-1) + \frac{e^{-\kappa(1-x)/x}}{x(1-x)} h(y) \right], \quad (23)$$

with  $N = N_\gamma/2$ ,  $\kappa = 2/3 \Upsilon$ . For the proposed luminosity we take the parameters  $\Upsilon = 8.1$ ,  $N_\gamma = 2.3$  [11]. The function  $h(y)$  is [33]

$$h(y) = \sum_{n=1}^{\infty} \frac{y^n}{n! \Gamma(n/3)}, \quad (24)$$

where  $y = N[\kappa(1-x)/x]^{1/3}$ . For large  $y$ ,  $h(y)$  has the asymptotic expansion

$$h(y) = \left( \frac{3z}{8\pi} \right)^{\frac{1}{2}} e^{4z} \left[ 1 - \frac{35}{288z} - \frac{1295}{16588z^2} + \dots \right], \quad (25)$$

with  $z = (y/3)^{3/4}$ .

In final states with  $\tau$  leptons, we select  $\tau$  decays to  $\pi$ ,  $\rho$  and  $a_1$  mesons (with a combined branching fraction of 54% [34]), in which a single  $\nu_\tau$  is produced, discarding other hadronic and leptonic decays. We simulate the  $\tau$  decay assuming that the meson and  $\tau$  momenta are collinear (what is a good approximation for high  $\tau$  energies) and assigning a random fraction  $x$  of the  $\tau$  momentum to the meson, according to the left-handed probability distributions [35]

$$P(x) = 2(1 - x) \quad (26)$$

for pions, and

$$P(x) = \frac{2}{2\zeta^3 - 4\zeta^2 + 1} [(1 - 2\zeta^2) - (1 - 2\zeta)x] \quad (27)$$

for  $\rho$  and  $a_1$  mesons, where  $\zeta = m_{\rho,a_1}^2/m_\tau^2$ . We assume a  $\tau$  jet tagging efficiency of 50%. In certain measurements the use of  $c$  tagging is necessary as well, and we assume a 50% efficiency, the same one that it is expected at ILC [36].

We simulate the calorimeter and tracking resolution of the detector by performing a Gaussian smearing of the energies of electrons ( $e$ ), muons ( $\mu$ ) and jets ( $j$ ), using the expected resolutions [12],

$$\frac{\Delta E^e}{E^e} = \frac{10\%}{\sqrt{E^e}} \oplus 1\% , \quad \frac{\Delta E^\mu}{E^\mu} = 0.005\% E^\mu , \quad \frac{\Delta E^j}{E^j} = \frac{50\%}{\sqrt{E^j}} \oplus 4\% , \quad (28)$$

where the two terms are added in quadrature and the energies are in GeV. We apply kinematical cuts on transverse momenta,  $p_T \geq 10$  GeV, and pseudorapidities  $|\eta| \leq 2.5$ , the latter corresponding to polar angles  $10^\circ \leq \theta \leq 170^\circ$ . We reject events in which the leptons or jets are not isolated, requiring a “lego-plot” separation  $\Delta R = \sqrt{\Delta\eta^2 + \Delta\phi^2} \geq 0.4$ . For the Monte Carlo integration in 6-body phase space we use **RAMBO** [37].

In electron and muon final states the light neutrino momentum  $p_\nu$  is determined from the missing transverse and longitudinal momentum of the event and the requirement that  $p_\nu^2 = 0$  (despite ISR and beamstrahlung, the missing longitudinal momentum approximates with a reasonable accuracy the original neutrino momentum). In final states with  $\tau$  leptons, the reconstruction is more involved, due to the secondary neutrino from the  $\tau$  decay. We determine the “primary” neutrino momentum and the

fraction  $x$  of the  $\tau$  momentum retained by the  $\tau$  jet using the kinematical constraints

$$\begin{aligned}
 E_W + E_\nu + \frac{1}{x}E_j &= \sqrt{s}, \\
 \vec{p}_W + \vec{p}_\nu + \frac{1}{x}\vec{p}_j &= 0, \\
 p_\nu^2 &= 0,
 \end{aligned}
 \tag{29}$$

in obvious notation. These constraints only hold if ISR and beamstrahlung are ignored, and in the limit of perfect detector resolution. When solving them for the generated Monte Carlo events we sometimes obtain  $x > 1$  or  $x < 0$ . In the first case we arbitrarily set  $x = 1$ , and in the second case we set  $x = 0.55$ , which is the average momentum fraction of the  $\tau$  jets. With the procedure outlined here, the reconstructed  $\tau$  momentum reproduces with a fair accuracy the original one, while the  $p_\nu$  obtained is often completely different from its actual value.

## 5 Heavy neutrino discovery at CLIC and determination of their properties

We address in turn the discovery of a new heavy neutrino (sections 5.1 and 5.2), the determination of its Dirac or Majorana character (section 5.3) and the measurement of its couplings to  $e$ ,  $\mu$ ,  $\tau$  (section 5.4). We try to be as concise as possible without losing generality or omitting the main points. Following the discussion in section 3 we can distinguish two interesting scenarios for our analysis: (*i*) the heavy neutrino only mixes with the electron; (*ii*) it mixes with  $e$  and either  $\mu$ ,  $\tau$ , or both. For the study of the  $m_N$  dependence and the determination of the neutrino nature we assume for simplicity that  $N$  only mixes with the electron. Additionally, we assume that the neutrino is a Majorana fermion in sections 5.1, 5.2 and 5.4, where the results obtained are almost independent of its character.

### 5.1 Discovery of a heavy neutrino

The existence of a heavy neutrino which couples to the electron can be detected as a sharp peak in the distribution of the  $ejj$  invariant mass  $m_{ejj}$ , plotted in Fig. 4 for  $V_{eN} = 0.05$ . The dotted and solid lines correspond to the SM and SM plus a 1500 GeV Majorana neutrino, respectively. For a Dirac neutrino the results do not change. The

width of the peak is mainly due to energy smearing included in our Monte Carlo, and the intrinsic  $N$  width,  $\Gamma_N = 8.2$  GeV and  $\Gamma_N = 4.1$  GeV for a Majorana and Dirac neutrino, respectively, has a smaller influence in this case.

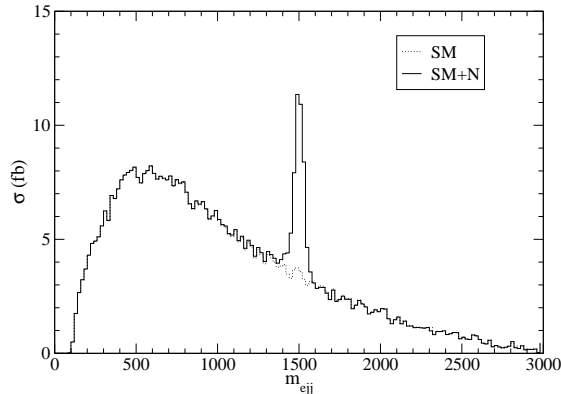


Figure 4: Kinematical distribution of the  $e+jj$  invariant mass, for  $m_N = 1500$  GeV.

The SM and SM plus heavy neutrino cross sections are collected in Table 1, before and after the kinematical cut

$$1460 \text{ GeV} \leq m_{ejj} \leq 1540 \text{ GeV} . \quad (30)$$

The criterion used here for the discovery of the new neutrino is that the excess of events<sup>3</sup> (the signal  $S$ ) in the peak region defined by Eq. (30) amounts to more than 5 standard deviations of the number of expected events (the background  $B$ ), that is,  $S/\sqrt{B} \geq 5$ . This ratio is larger than 5 for  $V_{eN} \geq 7.8 \times 10^{-3}$ , which is the minimum mixing angle for which a 1500 GeV neutrino can be discovered. Conversely, if no signal is found, the limit  $V_{eN} \leq 4.5 \times 10^{-3}$  can be set at 90% confidence level (CL), improving the present limit  $V_{eN} \leq 0.073$  by a factor of 16.

	No cut	With cut
SM	516	14.6
SM + $N$	548	39.4

Table 1: Cross sections (in fb) for  $e^+e^- \rightarrow e^\mp W^\pm \nu$  before and after the kinematical cut in Eq. (30).

---

<sup>3</sup>It must be stressed that the SM cross section at the peak can be calculated and normalised using the measurements far from this region.



In the most general case that  $N$  simultaneously mixes with the three charged leptons, there may be in principle signals in the  $e$ ,  $\mu$  and  $\tau$  channels, and the three of them must be experimentally analysed. We choose equal values  $V_{eN} = V_{\mu N} = V_{\tau N} = 0.04$  to illustrate the relative sensitivities of the three channels. For electron and muon final states we apply the kinematical cut in Eq. (30), while for taus the distribution is broader and we use

$$1420 \text{ GeV} \leq m_{\tau jj} \leq 1580 \text{ GeV}. \quad (31)$$

The SM and SM plus heavy neutrino cross sections after these kinematical cuts<sup>4</sup> can be found in Table 2. For these values of the couplings, the heavy neutrino signal could be seen with a statistical significance of  $\sim 40\sigma$ ,  $\sim 250\sigma$  and  $\sim 70\sigma$  in the  $e$ ,  $\mu$  and  $\tau$  channels, respectively, after one year of running.

	$e$	$\mu$	$\tau$
SM	14.6	0.36	0.096
SM + $N$	19.5	5.24	1.19

Table 2: Cross sections (in fb) for  $e^+e^- \rightarrow \ell^\mp W^\pm \nu$ , for  $\ell = e, \mu, \tau$ , including the kinematical cuts on  $m_{\ell jj}$ .

We clearly see that the muon channel is much more sensitive for equal values of the couplings. An  $eNW$  interaction is absolutely necessary to produce the heavy neutrino at observable rates but, once it has been produced, its decays in the muon and tau channels are easier to spot over the background. Since the production mechanism is strongly dominated by  $t$  and  $u$ -channel  $W$  exchange diagrams (see section 3), the observed signals  $S_e, S_\mu, S_\tau$  can be written as

$$S_\ell = A_\ell V_{eN}^2 \frac{V_{\ell N}^2}{V_{eN}^2 + V_{\mu N}^2 + V_{\tau N}^2} \quad (32)$$

to an excellent approximation. The common factor  $V_{eN}^2$  comes from the production, the ratio of couplings corresponds to the decay and  $A_\ell$  are constants. Using the data in Table 2 and Eqs. (32) we can obtain the combined limits on  $V_{eN}$  and  $V_{\mu N}$  or  $V_{\tau N}$  plotted in Fig. 5. It is very interesting to observe that a small coupling to the muon

---

<sup>4</sup>For the muon and tau channels the background is dominated by resonant  $W^+W^-$  production, thus a cut on the  $m_{\ell\nu}$  invariant mass could reduce it significantly. However, in practice it may be very difficult to reconstruct the  $W$  mass at CLIC energy, and to be conservative we do not apply any cut on  $m_{\ell\nu}$ .

$V_{\mu N} \gtrsim 0.005$  greatly increases the sensitivity to  $V_{eN}$ , from  $\sim 0.008$  to  $\sim 0.0035$ , due to the better observation of the heavy neutrino in the muon channel. For a fixed  $V_{eN}$  and increasing  $V_{\mu N}$ , the  $eW\nu$  channel becomes less significant because of the smaller branching ratio, and the observation is better in the  $\mu W\nu$  channel. (For ILC the behaviour is rather different, see next section.) In the case of the tau the effect is similar but less pronounced.

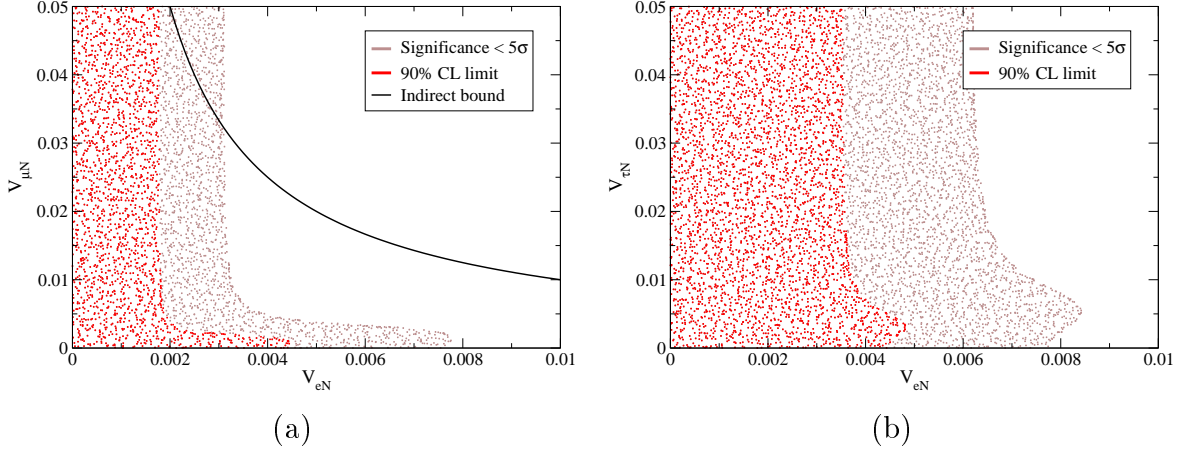


Figure 5: Combined limits on:  $V_{eN}$  and  $V_{\mu N}$ , for  $V_{\tau N} = 0$  (a);  $V_{eN}$  and  $V_{\tau N}$ , for  $V_{\mu N} = 0$  (b), for  $m_N = 1500$  GeV. The red areas represent the 90% CL limits if no signal is observed. The white areas extend up to present bounds  $V_{eN} \leq 0.073$ ,  $V_{\mu N} \leq 0.098$ ,  $V_{\tau N} \leq 0.13$ , and correspond to the region where a combined statistical significance of  $5\sigma$  or larger is achieved. The indirect limit from  $\mu - e$  LFV processes is also shown.

For comparison, we include in Fig. 5 (a) the indirect limit on  $V_{eN}$ ,  $V_{\mu N}$  derived from low energy LFV processes. For  $V_{\mu N}$  smaller than 0.05, the direct limit obtained by the absence of heavy neutrino production is much better than the indirect one. Moreover, the latter can be evaded if we allow for cancellations between heavy neutrino contributions, as discussed in section 2 (see also Ref. [10]). In the case of the tau lepton, the indirect limit from LFV processes is less stringent than the direct limits  $V_{eN} \leq 0.073$ ,  $V_{\tau N} \leq 0.13$  and is not shown.

When the heavy neutrino does not couple to the electron but only to the muon and/or tau, the only Feynman diagram contributing to the signal is 3c. For CLIC the situation is much worse than for ILC [10] because at a higher CM energy this diagram is more suppressed. Heavy neutrino production rates are thus negligibly small, giving an excess of a handful of events (for an integrated luminosity of  $1000 \text{ fb}^{-1}$ ) over the

SM background even for  $V_{\mu N}, V_{\tau N}$  in their upper experimental bounds.

## 5.2 Dependence on the heavy neutrino mass

The cross section for  $e^+e^- \rightarrow e^\mp W^\pm \nu$  including the heavy neutrino contribution exhibits a moderate dependence on  $m_N$ , which is mainly due to phase space. The variation of the total  $e^\mp W^\pm \nu$  cross section (including ISR, beamstrahlung and “detector cuts” as explained in section 4) with  $m_N$  can be seen in Fig. 6 (a). For larger masses the cross sections are smaller and thus the limits on  $V_{eN}$  are worse. This behaviour is attenuated by the fact that the SM background also decreases for larger  $m_{e\bar{e}j}$ , as can be clearly observed in Fig. 4. The resulting limits on the heavy neutrino coupling are shown in Fig. 6 (b) as a function of  $m_N$ . These limits assume implicitly that the heavy neutrino only mixes with the electron (for mixing also with the muon they improve, as seen in the previous subsection). The kinematical cuts are not optimised for each value of  $m_N$ .

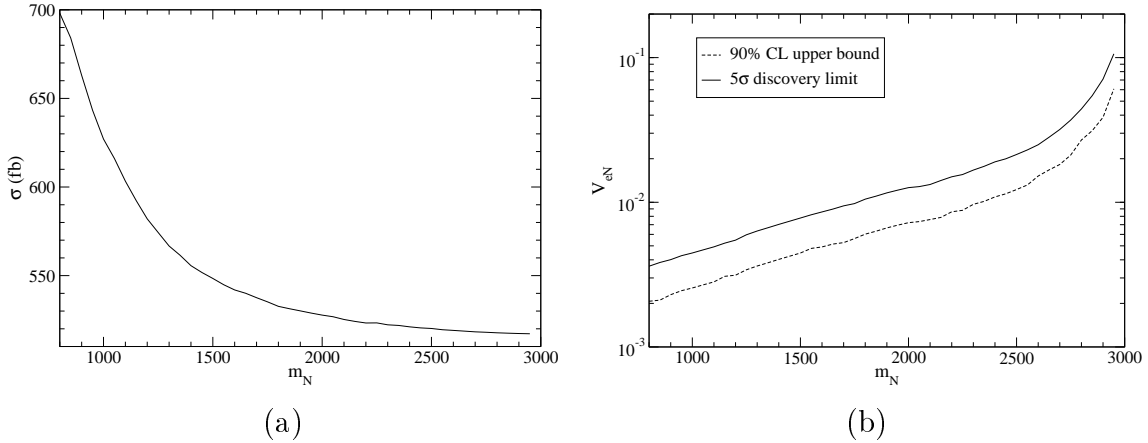


Figure 6: (a) Cross section for  $e^+e^- \rightarrow e^\mp W^\pm \nu$  for  $V_{eN} = 0.05$  and different values of  $m_N$ . (b) Dependence of the discovery and upper limits on  $V_{eN}$  on the heavy neutrino mass. Both plots assume mixing only with the electron.

## 5.3 Determination of the Majorana or Dirac nature

The cross section for  $e^-W^+\nu$  production mediated by a heavy neutrino is fairly insensitive to its Dirac or Majorana character. Still, the different production mechanisms show up in the angular distribution of  $N$  with respect to the incoming electron. In

the case of a heavy Majorana neutrino the new contribution is dominated by diagrams 1a, 1b, leading to a forward-backward symmetric distribution for the production angle  $\varphi_{Ne^-}$  between  $N$  and the incoming electron. The distribution peaks at  $\cos \varphi_{Ne^-} = 1$  when  $t \equiv (p_N - p_{e^-})^2 = 0$  and the first diagram is enhanced, and at  $\cos \varphi_{Ne^-} = -1$  when  $u \equiv (p_N - p_{e^+})^2 = 0$  (and the second one is enhanced).

In the case of Dirac neutrinos the  $u$ -channel diagram is absent, and the distribution only peaks at  $\cos \varphi_{Ne^-} = 1$  for final states with  $e^-, \mu^-, \tau^-$  and at  $\cos \varphi_{Ne^-} = -1$  for the charge conjugate processes with  $e^+, \mu^+, \tau^+$ . It is then convenient to define  $\varphi_N \equiv \varphi_{Ne^-}, \varphi_{Ne^+}$  for  $e^-W^+\nu, e^+W^-\nu$  events, respectively. Its normalised distribution is shown in Fig. 7 (a) for events surviving the kinematical cut in Eq. (30). We consider the SM, and SM plus a Majorana or Dirac neutrino. The most conspicuous results are obtained subtracting the SM contribution, which can be calculated and calibrated using the measurements outside the peak. In this case, Fig. 7 (b), the difference between the Dirac and Majorana cases is apparent. We remark that the signal cross section at the peak is of 24.8 fb for  $V_{eN} = 0.05$ , what gives a sufficiently large event sample to distinguish both cases even for smaller mixing angles (see also Fig. 6).

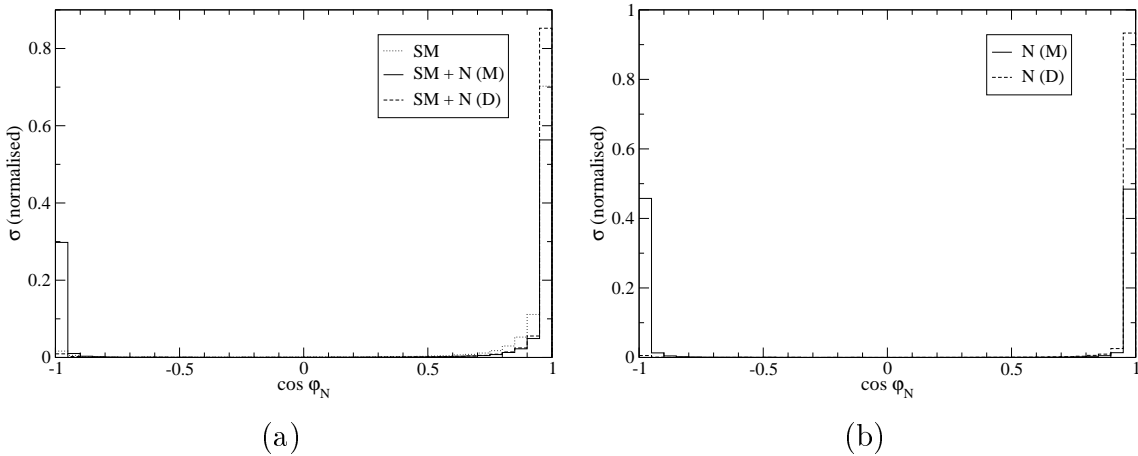


Figure 7: (a) Dependence of the cross section on the angle  $\varphi_N$ , for the SM and the SM plus a 1500 GeV Majorana (M) or Dirac (D) neutrino. (b) The same, but subtracting the SM contribution.

For completeness, we also show in Fig. 8 the dependence of the cross section on the angles  $\varphi_W, \varphi_e$  between the produced  $W^\pm, e^\mp$  and the incoming electron (for  $e^-$  final states) or positron (for final  $e^+$ ). We restrict ourselves to events surviving the kinematical cut in Eq. (30), as in the previous case. Although these two distributions also show some sensitivity to the Dirac or Majorana character of the neutrino, it is

obvious when compared to Fig. 7 (a) that the best results are obtained from the analysis of the polar angle of the produced neutrino  $\varphi_N$ .

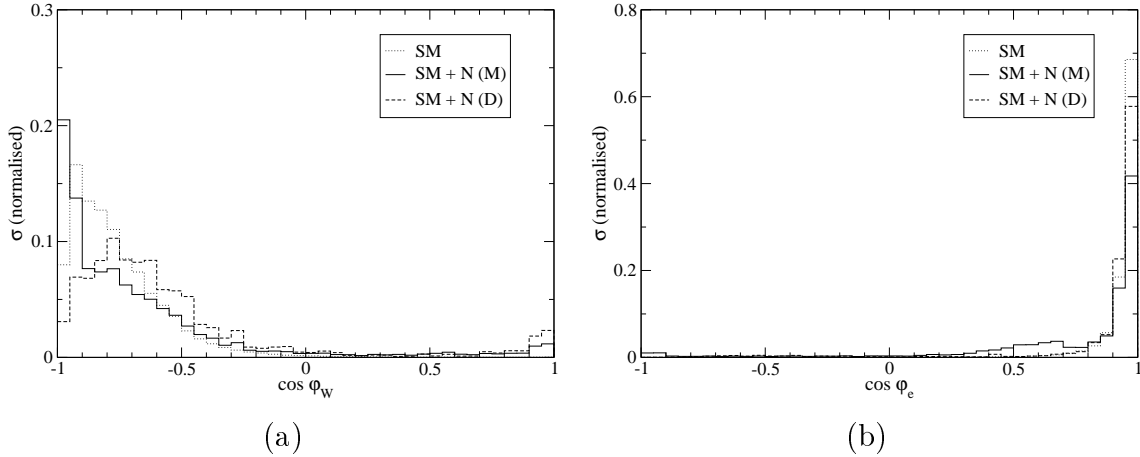


Figure 8: Dependence of the cross section on the angles  $\varphi_W$  (a) and  $\varphi_e$  (b), for the SM and the SM plus a 1500 GeV Majorana or Dirac neutrino.

## 5.4 Measurement of heavy neutrino couplings

In order to measure the moduli of the heavy neutrino couplings to charged leptons, the constants  $A_\ell$  in Eq. (32) must be theoretically calculated. This can be done in principle with full Monte Carlo simulations taking into account all radiation and hadronisation effects, as well as the real detector behaviour. The couplings of the heavy neutrino are then

$$\begin{aligned}
 V_{eN}^2 &= \frac{S_e}{A_e} + \frac{S_\mu}{A_\mu} + \frac{S_\tau}{A_\tau}, \\
 \frac{V_{\ell N}^2}{V_{eN}^2} &= \frac{S_\ell}{A_\ell} \left( \frac{S_e}{A_e} \right)^{-1}, \quad \ell = \mu, \tau.
 \end{aligned} \tag{33}$$

The uncertainty in their measurement comes from the statistical fluctuations of the signal and background, as well as from the theoretical calculation of the constants  $A_\ell$ . Among other factors, their calculation is affected by the inherent uncertainties in the signal normalisation. We expect that  $A_\ell$  can be obtained with a precision of 10%, which in principle does not affect the determination of coupling ratios.

We estimate the accuracy with which heavy neutrino couplings could be extracted, calculating the  $A_\ell$  constants from the peak cross sections given by our Monte Carlo for a

“reference” set of couplings, and assuming a common 10% error in their determination. Then, using as input the cross sections for  $V_{eN} = V_{\mu N} = V_{\tau N} = 0.04$ , the couplings obtained are

$$\begin{aligned} V_{eN} &= 0.0388 \pm 0.00034 \text{ (stat)} \pm 0.0019 \text{ (sys)}, \\ V_{\mu N}/V_{eN} &= 1.007 \pm 0.016 \text{ (stat)}, \\ V_{\tau N}/V_{eN} &= 1.030 \pm 0.028 \text{ (stat)}. \end{aligned} \tag{34}$$

In this case the statistical precision of the ratios is very good, of a 2 – 3%. The uncertainty in  $V_{eN}$  is of a 5%, dominated by systematics.

A second issue is the determination of the chirality of  $\ell NW$  couplings. This can be done with the measurement of the  $\ell s$  forward-backward (FB) asymmetry in the  $W$  rest frame [38, 39], which is sensitive to the chiral structure of the  $\ell NW$  coupling involved in the decay  $N \rightarrow \ell^- W^+ \rightarrow \ell^- c \bar{s}$  (and in its charge conjugate). The measurement of this asymmetry requires to distinguish between the two quark jets resulting from  $W^+$  decay, what can be done restricting ourselves to  $W^+ \rightarrow c \bar{s}$  and taking advantage of  $c$  tagging to require a tagged  $c$  jet in the final state. This reduces the cross sections by a factor of four.

We define  $\theta_{\ell s}$  as the angle between the momenta of the charged lepton  $\ell$  and the  $\bar{s}$  jet, in the  $W$  rest frame (the definition is the same for  $N$  decays into  $\ell^- W^+ \rightarrow \ell^- c \bar{s}$  and  $\ell^+ W^- \rightarrow \ell^+ c \bar{s}$ ). The FB asymmetry is defined as

$$A_{\text{FB}} = \frac{N(\cos \theta_{\ell s} > 0) - N(\cos \theta_{\ell s} < 0)}{N(\cos \theta_{\ell s} > 0) + N(\cos \theta_{\ell s} < 0)}, \tag{35}$$

with  $N$  standing for the number of events. If we parameterise a general  $\ell NW$  vertex (ignoring effective  $\sigma^{\mu\nu}$  terms) as

$$\mathcal{L}_{\ell WN} = -\frac{g}{\sqrt{2}} \bar{\ell} \gamma^\mu (g_L P_L + g_R P_R) N W_\mu + \text{H.c.} \tag{36}$$

and assume that the  $W$  coupling to quarks is purely left-handed, the FB asymmetry is

$$A_{\text{FB}} = \frac{3M_W^2}{4M_W^2 + 2m_N^2} \frac{|g_L|^2 - |g_R|^2}{|g_L|^2 + |g_R|^2}. \tag{37}$$

In the case of heavy neutrino singlets  $g_L = V_{\ell N}$ ,  $g_R = 0$  as seen in Eq. (14), and the second factor in Eq. (37) equals unity. Still, the first factor is very small for  $m_N \gg M_W$ , and for  $m_N = 1500$  GeV we have  $A_{\text{FB}} = 4.3 \times 10^{-3}$  for the three lepton flavours. Such asymmetries are unobservable, as long as the experimental statistical errors expected

in the experiment are typically  $\Delta A_{\text{FB}} \gtrsim 0.012$ .<sup>5</sup> Still, for  $m_N$  of several hundreds of GeV the asymmetries are measurable. We analyse such possibility in next section.

Further observables are sensitive to the structure of the  $\ell NW$  vertices, namely spin asymmetries. A proper analysis requires the search for a direction along which the  $N$  polarisation is maximal, what is beyond the scope of this work. Besides, the information on couplings extracted from such observables is expected to be less clean, since they involve additional variables apart from masses and couplings.

## 6 Heavy non-decoupled neutrinos at ILC

Heavy neutrinos with masses up to a few hundreds of GeV can also be produced at ILC with a CM energy of 500 GeV. Many features of the production process are common to both mass and CM energy scales, but in some other respects ILC and CLIC are rather different. In order to have a better comparison between both cases we summarise here several results for ILC extending the work in Ref. [10]. We take a mass  $m_N = 300$  GeV for most of our computations, which follow closely what is done for CLIC (see also Ref. [10] for details). The integrated luminosity is assumed to be  $345 \text{ fb}^{-1}$ , corresponding to one year of running.

With the same signal reconstruction method as for CLIC we obtain for  $m_N = 300$  GeV the combined limits on  $V_{eN}$  and  $V_{\mu N}$  or  $V_{\tau N}$  plotted in Fig. 9. In contrast with the behaviour obtained at CLIC, at ILC the sensitivities in the muon and electron channels are similar, and both are better than in  $\tau W \nu$  production. This can be clearly observed in both plots: a  $\mu NW$  coupling has little effect on the limits on  $V_{eN}$ , but a coupling with the tau decreases the sensitivity, because the decays in the tau channel are harder to observe. The direct limit on  $V_{eN}$ ,  $V_{\mu N}$  obtained here improves the indirect one only for  $V_{\mu N} \lesssim 0.01$ . However, as it has already been remarked, the latter is not general and can be evaded with cancellations among heavy neutrino contributions [10].

The dependence of the total  $e^\pm W^\pm \nu$  cross section on  $m_N$  can be seen in Fig. 10 (a), for  $V_{eN} = 0.073$ ,  $V_{\mu N} = V_{\tau N} = 0$ . For a heavier  $N$  the cross sections are smaller and thus the limits on  $V_{eN}$  are worse. However, up to  $m_N = 400$  GeV this is compensated

---

<sup>5</sup>In the absence of background, the statistical error of an asymmetry  $A$  is given by the simple expression  $\Delta A = \sqrt{(1 - A^2)/(SL)}$ , with  $S$  the signal cross section and  $L$  the integrated luminosity. With an asymmetric background the expression is more involved but it can be seen that  $\Delta A$  is larger than without background.

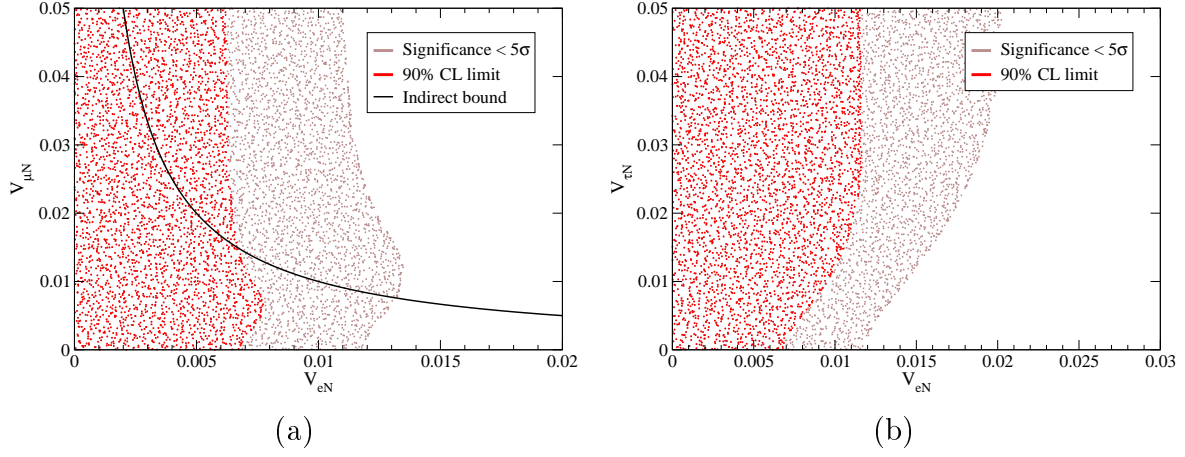


Figure 9: Combined limits obtained at ILC on:  $V_{eN}$  and  $V_{\mu N}$ , for  $V_{\tau N} = 0$  (a);  $V_{eN}$  and  $V_{\tau N}$ , for  $V_{\mu N} = 0$  (b). The red areas represent the 90% CL limits if no signal is observed. The white areas extend up to present bounds  $V_{eN} \leq 0.073$ ,  $V_{\mu N} \leq 0.098$ ,  $V_{\tau N} \leq 0.13$ , and correspond to the region where a combined statistical significance of  $5\sigma$  or larger is achieved. The indirect limit from  $\mu - e$  LFV processes is also shown. We take  $m_N = 300$  GeV.

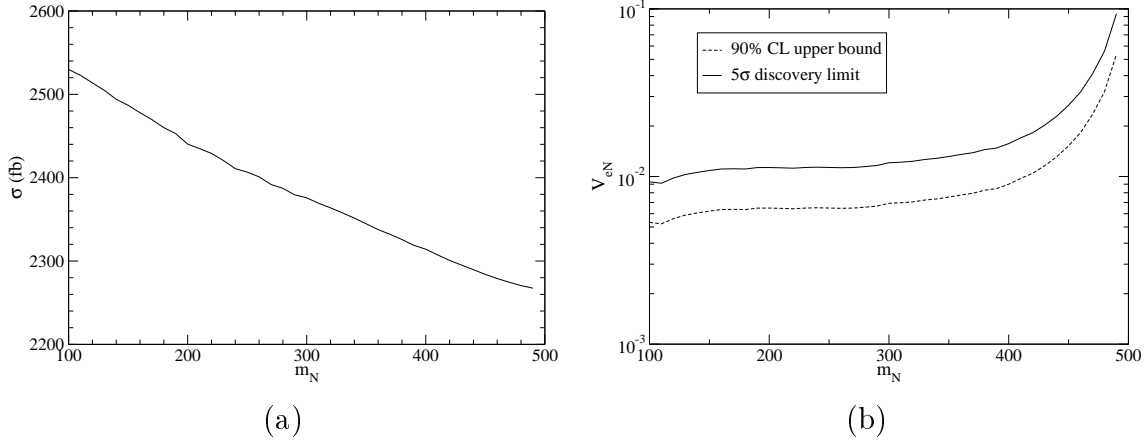


Figure 10: (a) Cross section for  $e^+e^- \rightarrow e^\mp W^\pm \nu$  at ILC for  $V_{eN} = 0.073$  and different values of  $m_N$ . (b) Dependence of the discovery and upper limits on  $V_{eN}$  on the heavy neutrino mass. Both plots assume mixing only with the electron.

by the fact that the SM background also decreases for larger  $m_{ejj}$ . The limits on  $V_{eN}$  are shown in Fig. 10 (b) as a function of  $m_N$ , assuming that the heavy neutrino only mixes with the electron.



If a heavy neutrino is discovered at ILC, its nature can be uniquely determined with the study of the  $\varphi_N$  dependence of the cross section, as it has been discussed in section 5.3. The dependence of the peak cross section on  $\varphi_N$  is shown in Fig. 11 (a). The results after subtracting the SM contribution can be seen in Fig. 11 (b). The distribution is less concentrated at  $\cos\varphi_N = \pm 1$  than for CLIC energy but allows to determine unambiguously the neutrino character even if a relatively small number of signal events is collected. The dependence of the peak cross section on  $\varphi_W$  and  $\varphi_e$  is presented in Fig. 12.<sup>6</sup>

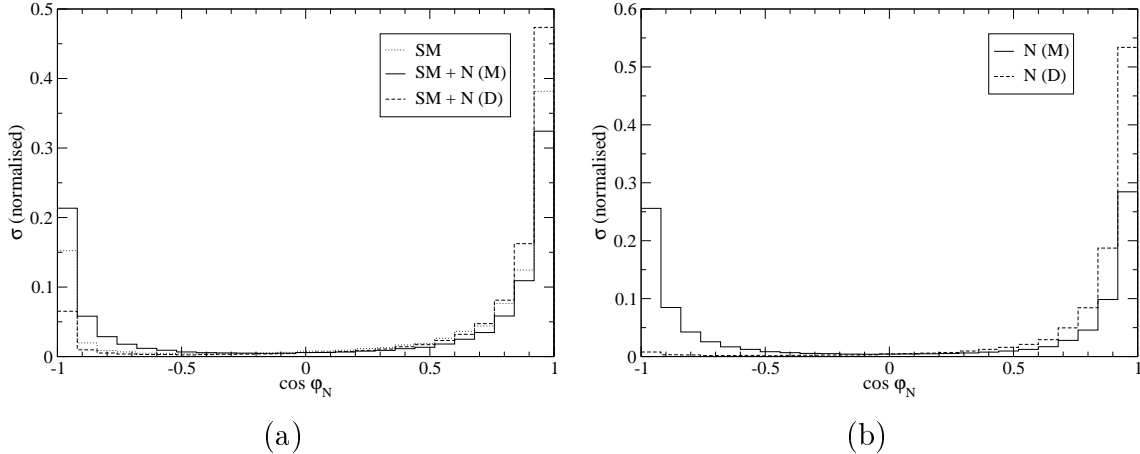


Figure 11: (a) Dependence of the cross section at ILC on the angle  $\varphi_N$ , for the SM and the SM plus a 300 GeV Majorana (M) or Dirac (D) neutrino. (b) The same, but subtracting the SM contribution.

The measurement at ILC of the  $V_{eN}$ ,  $V_{\mu N}$ ,  $V_{\tau N}$  moduli can be done in the same way described for CLIC, without any substantial differences, thus we do not repeat that discussion here. Still, an important difference appears in the determination of their chiral structure. In contrast with TeV scale neutrinos, for  $m_N = 300$  GeV the FB asymmetry is observable. We show in Fig. 13 (a) the dependence of the SM and SM plus heavy neutrino peak cross sections with respect to the angle  $\theta_{es}$ . The measurement of the FB asymmetry requires the subtraction of the SM prediction, giving the distributions shown in Fig. 13 (b). For a Majorana neutrino with  $V_{eN} = 0.073$ ,  $V_{\mu N} = V_{\tau N} = 0$ , the resulting asymmetry is  $A_{\text{FB}} = 0.083 \pm 0.016$ , where the error quoted is statistical. The SM and SM+N cross sections after  $c$  tagging are 13.4 and 32.7 fb, including only  $W$  hadronic decays with a  $c$  quark. For a Dirac neutrino the results

<sup>6</sup>It should be noted that the  $\varphi_W$  and  $\varphi_e$  distributions presented in Ref. [10] correspond to the whole range of  $m_{ejj}$  and not only to the peak.

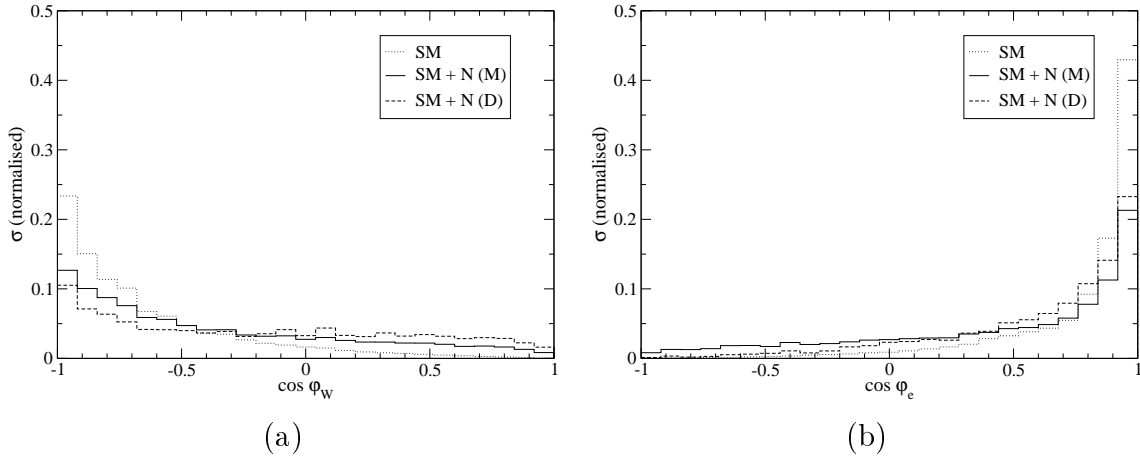


Figure 12: Dependence of the cross section at ILC on the angles  $\varphi_W$  (a) and  $\varphi_e$  (b), for the SM and the SM plus a 300 GeV Majorana or Dirac neutrino.

found are equivalent within Monte Carlo uncertainty. The FB asymmetry obtained from the simulation is in good agreement with the theoretical value  $A_{\text{FB}} = 0.094$  expected for a purely left-handed coupling.

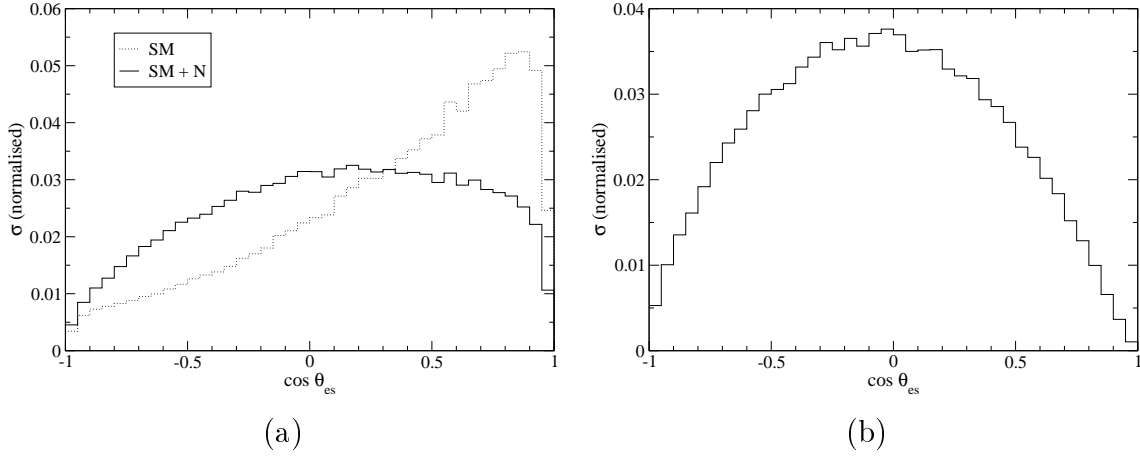


Figure 13: (a) Dependence of the cross section at ILC on the angle  $\theta_{es}$  for the SM and the SM plus a 300 GeV Majorana neutrino. (b) The same, but subtracting the SM contribution.

If a heavy neutrino signal is observed in this mass range, we expect that the FB asymmetry will have a sufficient statistical significance so as to indicate that the  $eNW$  coupling is left-handed, at least after several years of running. The precision of the  $A_{\text{FB}}$  measurement strongly depends on the size of the  $N$  cross section, therefore the

possibility of extracting the left- and right-handed parts of the coupling from the total cross section and  $A_{\text{FB}}$  measurements is difficult to assess in general.

## 7 Conclusions

Neutrinos with masses of the order of 1 TeV are predicted by many models attempting to make the new physics scale observable at future colliders. Their presence leads to a greater complexity of the models (in order to reproduce the light neutrino masses), especially when they are not decoupled from the light fermions. Nevertheless, if they exist, large  $e^+e^-$  colliders can discover them or provide the best limits on their masses and mixings. Such discovery would give a new insight into the mechanism for neutrino mass generation.

In this paper we have concentrated on the production of heavy neutrino singlets in association with a light neutrino. If they are the only addition to the SM, the production cross section for  $NN$  pairs is suppressed by extra mixing angle factors  $V_{\ell N}^2$ . This is also reduced by the smaller phase space and by additional decay branching ratios, what makes this process much less sensitive to the presence of these heavy fermions.<sup>7</sup> In left-right models the new gauge interactions allow to produce heavy neutrinos in pairs, or in association with charged leptons, with mixing angles of order unity. LHC will be sensitive to both mechanisms [40], but the most stringent limits are expected from the latter processes [41, 42]. On the other hand,  $e^+e^-$  colliders will be mainly sensitive to neutrino pair production [12, 43], which might be used to learn about heavy neutrino properties as well [44]. We note that in the case of Majorana neutrinos,  $NN$  production may give an interesting lepton number violating final state signal  $NN \rightarrow \ell^\pm W^\mp \ell'^\pm W^\mp$  [26, 45], which has smaller backgrounds than the analogous lepton number conserving final state  $\ell^\pm W^\mp \ell'^\mp W^\pm$ . In case that new interactions are pushed to high energies, heavy neutral leptons can still be produced in pairs if they transform non-trivially under the SM gauge group [25].

We have discussed the prospects for TeV scale neutrino detection in  $\ell W \nu$  production at future  $e^+e^-$  colliders, taking as example the CLIC proposal for a 3 TeV collider at

---

<sup>7</sup>For  $e^+e^- \rightarrow NN$  the  $t$  and  $u$ -channel exchange diagrams are quadratic in  $V_{eN}$ , and the  $s$ -channel  $Z$  diagram has the mixing factor  $X_{NN}$  in Eq. (8), which is equal to  $|V_{eN}|^2 + |V_{\mu N}|^2 + |V_{\tau N}|^2$ . Therefore, the cross section is proportional to light-heavy mixing angles to the fourth power. For  $m_N = 1$  TeV and a coupling  $V_{eN} = 0.004$  in the discovery limit, the extra mixing angle suppression of this cross section is of order  $V_{eN}^2 = 1.6 \times 10^{-5}$ , already giving unobservable rates for heavy neutrino pair production.

CERN. This study complements the analysis of the CLIC potential based on new gauge interactions [12, 43]. We have examined the dependence of the results on the heavy neutrino mass, and special emphasis has been made on the importance of a complete study of the three possible channels  $\ell = e, \mu, \tau$ . As it has been argued, a non-negligible coupling to the electron,  $V_{eN} \sim 10^{-3} - 10^{-2}$  for  $m_N = 1 - 2$  TeV, is necessary to produce the heavy neutrino at detectable rates. The produced neutrinos can then decay  $N \rightarrow eW$  and, if they couple to the muon and tau,  $N \rightarrow \mu W$  and  $N \rightarrow \tau W$  as well (plus additional decays mediated by neutral currents). Among these, the muon channel is by far the cleanest one due to its smaller background. We have explicitly shown that for  $m_N = 1500$  GeV the sensitivity to  $V_{eN}$  improves from  $V_{eN} \sim 0.008$  to  $V_{eN} \sim 0.0035$  in the presence of a small coupling  $V_{\mu N} \sim 0.005$ , but is hardly affected by  $N$  mixing with the tau lepton.

We have also studied what we could learn about heavy neutrinos if they were discovered at CLIC. It has been shown that the angular distribution of the produced neutrino relative to the beam axis is a powerful discriminant between Majorana and Dirac neutrinos, giving a clear evidence of their nature even for relatively small signals. Then, we have discussed how to extract heavy neutrino charged current couplings from data, estimating with an example the precision with which they could be eventually measured. We have proposed a method to determine the chiral structure of the  $\ell NW$  interactions, which unfortunately is only useful for neutrino masses below the TeV scale.

Finally, we have performed a similar analysis for heavy neutrinos of few hundreds of GeV at ILC, extending a recent analysis [10]. In particular, we have explicitly investigated the flavour and mass dependence of the limits on neutrino mixing with charged leptons. For a heavy neutrino with a mixing large enough, we have shown how to establish its Dirac or Majorana nature and how to determine the chirality of its charged current couplings.

The results obtained show that CLIC would outperform previous machines in finding direct or indirect signals of heavy neutrinos. It would extend direct searches up to masses around 2.5 TeV, and for masses around 1 TeV it would be sensitive to couplings  $V_{eN} \simeq 4 \times 10^{-3}$ . If no heavy neutrino signal was found at CLIC, the bound  $V_{eN} \leq 2 - 6 \times 10^{-3}$  could be set for  $m_N = 1 - 2$  TeV, improving the present limit  $V_{eN} \leq 0.073$  by more than one order of magnitude and matching a future limit obtained at the GigaZ option of ILC [46], for which a  $10^3$  statistical gain would be expected to translate into bounds  $\sim 30$  times more stringent than those of Eqs. (12).

The direct limit on the product  $V_{eN}V_{\mu N}^*$  obtained from the non-observation of heavy neutrinos would be much more restrictive than the present indirect bound from LFV processes, and would remain competitive with future improvements of the upper bounds on  $\text{Br}(\mu \rightarrow e\gamma)$  [47] and  $\mu - e$  conversion in nuclei [48]. For heavy neutrinos with masses of few hundreds of GeV, CLIC would probe mixing angles  $V_{eN} \sim 10^{-3}$ , one order of magnitude better than what will be achieved at ILC.

## Acknowledgements

F.A. thanks J. Bernabéu, A. Bueno, J. Wudka and M. Zralek for discussions. J.A.A.S. thanks F. R. Joaquim for useful comments. This work has been supported in part by MEC and FEDER Grant No. FPA2003-09298-C02-01, by Junta de Andalucía Group FQM 101, by FCT through projects POCTI/FNU/44409/2002, CFTP-FCT UNIT 777 and grant SFRH/BPD/12603/2003, and by the European Community's Human Potential Programme under contract HPRN-CT-2000-00149 Physics at Colliders.

## References

- [1] P. Minkowski, Phys. Lett. B **67** (1977) 421; M. Gell-Mann, P. Ramond and R. Slansky in *Supergravity*, p. 315, edited by F. Nieuwenhuizen and D. Friedman, North Holland, Amsterdam, 1979; T. Yanagida, Proceedings of the *Workshop on Unified Theories and Baryon Number of the Universe*, edited by O. Sawada and A. Sugamoto, KEK, Japan 1979; R.N. Mohapatra and G. Senjanovic, Phys. Rev. Lett. **44** (1980) 912
- [2] M. Fukugita and T. Yanagida, Phys. Lett. B **174** (1986) 45; for a recent review and references see W. Buchmüller, P. Di Bari and M. Plümacher, Annals Phys. **315** (2005) 305
- [3] L. Boubekur, T. Hambye and G. Senjanovic, Phys. Rev. Lett. **93** (2004) 111601; A. Abada, H. Aissaoui and M. Losada, hep-ph/0409343
- [4] A. Pilaftsis and T. E. J. Underwood, Nucl. Phys. B **692** (2004) 303; T. Hambye, J. March-Russell and S. M. West, JHEP **0407** (2004) 070; R. Gonzalez Felipe, F. R. Joaquim and B. M. Nobre, Phys. Rev. D **70** (2004) 085009

- [5] J. Gluza, Acta Phys. Polon. B **33** (2002) 1735; for a review and a list of references see G. Altarelli and F. Feruglio, New J. Phys. **6** (2004) 106
- [6] See for instance B. Bekman, J. Gluza, J. Holeczek, J. Syska and M. Zralek, Phys. Rev. D **66** (2002) 093004
- [7] For a review and references see J. L. Hewett and T. G. Rizzo, Phys. Rept. **183** (1989) 193
- [8] M. J. Bowick and P. Ramond, Phys. Lett. B **103** (1981) 338; F. del Aguila and M. J. Bowick, Nucl. Phys. B **224** (1983) 107
- [9] F. del Aguila and J. Santiago, JHEP **0203** (2002) 010; for a review see also F. Feruglio, Eur. Phys. J. C **33** (2004) S114; C. Csáki, hep-ph/0404096
- [10] F. del Aguila, J. A. Aguilar-Saavedra, A. Martínez de la Ossa and D. Meloni, Phys. Lett. B **613** (2005) 170
- [11] R. W. Assmann *et al.* [The CLIC Study Team], CERN 2000-008
- [12] E. Accomando *et al.* [CLIC Physics Working Group], hep-ph/0412251.
- [13] B. Pontecorvo, Sov. Phys. JETP **6** (1958) 429; Z. Maki, M. Nakagawa and S. Sakata, Prog. Theor. Phys. **28** (1962) 870
- [14] G.C. Branco, L. Lavoura and J.P. Silva, *CP Violation*, Oxford University Press, Oxford, UK (1999); R.N. Mohapatra and P.B. Pal, *Massive neutrinos in physics and astrophysics: second edition* World Sci. Lect. Notes Phys. **72** (2004) 1
- [15] P. Langacker and D. London, Phys. Rev. D **38** (1988) 907
- [16] J. G. Korner, A. Pilaftsis and K. Schilcher, Phys. Lett. B **300** (1993) 381
- [17] E. Nardi, E. Roulet and D. Tommasini, Phys. Lett. B **327** (1994) 319
- [18] A. Ilakovac and A. Pilaftsis, Nucl. Phys. B **437** (1995) 491
- [19] D. Tommasini, G. Barenboim, J. Bernabeu and C. Jarlskog, Nucl. Phys. B **444** (1995) 451
- [20] S. Bergmann and A. Kagan, Nucl. Phys. B **538** (1999) 368
- [21] J. I. Illana and T. Riemann, Phys. Rev. D **63** (2001) 053004

- [22] J. Gluza and M. Zralek, Phys. Rev. D **55** (1997) 7030; see also J. Gluza and M. Zralek, Phys. Rev. D **48** (1993) 5093
- [23] R.N. Mohapatra, Nucl. Phys. Proc. Suppl. **77** (1999) 376; for a recent review see C. Aalseth *et al.*, hep-ph/0412300
- [24] A. Pilaftsis, Z. Phys. C **55** (1992) 275
- [25] F. del Aguila, E. Laermann and P. Zerwas, Nucl. Phys. B **297** (1988) 1; W. Buchmuller and C. Greub, Nucl. Phys. B **363** (1991) 345; G. Azuelos and A. Djouadi, Z. Phys. C **63** (1994) 327
- [26] J. Maalampi, K. Mursula and R. Vuopionpera, Nucl. Phys. B **372** (1992) 23
- [27] G. Eilam, J. L. Hewett and A. Soni, Phys. Rev. Lett. **67** (1991) 1979
- [28] J. A. Aguilar-Saavedra, hep-ph/0410068, Nucl. Phys. B (in press)
- [29] E. Murayama, I. Watanabe and K. Hagiwara, KEK report 91-11, January 1992
- [30] A. Denner, H. Eck, O. Hahn and J. Kublbeck, Nucl. Phys. B **387** (1992) 467
- [31] M. Skrzypek and S. Jadach, Z. Phys. C **49** (1991) 577
- [32] M. Peskin, Linear Collider Collaboration Note LCC-0010, January 1999
- [33] K. Yokoya and P. Chen, SLAC-PUB-4935. *Presented at IEEE Particle Accelerator Conference, Chicago, Illinois, Mar 20-23, 1989*
- [34] S. Eidelman *et al.* [Particle Data Group], Phys. Lett. B **592** (2004) 1
- [35] J. D. Anderson, M. H. Austern and R. N. Cahn, Phys. Rev. D **46** (1992) 290
- [36] S. M. Xella Hansen, C. Damerell, D. J. Jackson and R. Hawkings, *Prepared for 5th International Linear Collider Workshop (LCWS 2000), Fermilab, Batavia, Illinois, 24-28 Oct 2000*
- [37] R. Kleiss, W. J. Stirling and S. D. Ellis, Comput. Phys. Commun. **40** (1986) 359
- [38] B. Lampe, Nucl. Phys. B **454** (1995) 506
- [39] F. del Aguila and J. A. Aguilar-Saavedra, Phys. Rev. D **67** (2003) 014009
- [40] A. Datta, M. Guchait and A. Pilaftsis, Phys. Rev. D **50** (1994) 3195

- [41] G. Weiglein *et al.* [LHC/LC Study Group], hep-ph/0410364.
- [42] A. Ferrari *et al.*, Phys. Rev. D **62** (2000) 013001
- [43] A. Ferrari, Phys. Rev. D **65** (2002) 093008
- [44] J. Kogo and S. Y. Tsai, Prog. Theor. Phys. **86** (1991) 183; A. Höfer and L. M. Sehgal, Phys. Rev. D **54** (1996) 1944
- [45] G. Cvetič, C. S. Kim and C. W. Kim, Phys. Rev. Lett. **82** (1999) 4761; see also E. Ma and J. T. Pantaleone, Phys. Rev. D **40** (1989) 2172
- [46] J. A. Aguilar-Saavedra *et al.* [ECFA/DESY LC Physics Working Group Collaboration], hep-ph/0106315
- [47] T. Mori, Nucl. Phys. Proc. Suppl. **111** (2002) 194; see also <http://meg.web.psi.ch/>
- [48] M. Hebert [MECO Collaboration], Nucl. Phys. A **721** (2003) 461; see also <http://meco.ps.uci.edu/>